# Multiple-Bond Correlations in Heteronuclear ND NMR

Analysis of *J*-coupling, especially ^{1}H-^{1}H *J*-couplings, both in terms of their precise values and the splitting patterns produced in 1D spectra, as well as the distinctive patterns that arise in multidimensional spectra form the basis of structural analysis using NMR.

Although direct heteronuclear couplings, $^1J_{HC}$ may be interpreted in a structural context, such correlations are fairly weak.

It was recognized early that heteronuclear couplings could provide valuable structural information in the same way that ^{1}H-^{1}H couplings do, and studies of compounds uniformly enriched in ^{13}C, readily reveal geminal and vicinal J_{CC}-couplings ($^1J_{CC} \approx 35$ Hz, $^{2,3}J_{CC} < 5$ Hz)

Observation of J_{CC} at the natural abundance level (1.1% ^{13}C) is complicated by the very low probability of finding adjacent ^{13}C nuclei, regardless of whether we are thinking of any of the following arrangements:

$$^{13}C-^{13}C-^{12}C-^{12}C$$

$$^{13}C-^{12}C-^{13}C-^{12}C$$

$$^{13}C-^{12}C-^{12}C-^{13}C$$
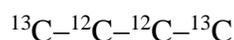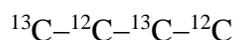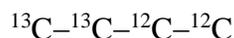
Nevertheless, such interactions do exist and by exploiting the production of multiple-quantum coherent states, $^1J_{CC}$, $^2J_{CC}$ and $^3J_{CC}$ couplings can be observed.

Recall that an *n*-quantum state can only be produced from *n* or more spins, thus the approach employed seeks to distinguish the two-spin ^{13}C systems from the isolated ^{13}C spins.

INADEQUATE: Incredible Natural Abundance Double Quantum Transfer Experiment

Bax, A., Freeman, R. and Kempsell, S.P. (1980) Natural Abundance $^{13}C–^{13}C$ Coupling Observed via Double-Quantum Coherence. *J. Am. Chem. Soc.* **102**, 4849-4851.

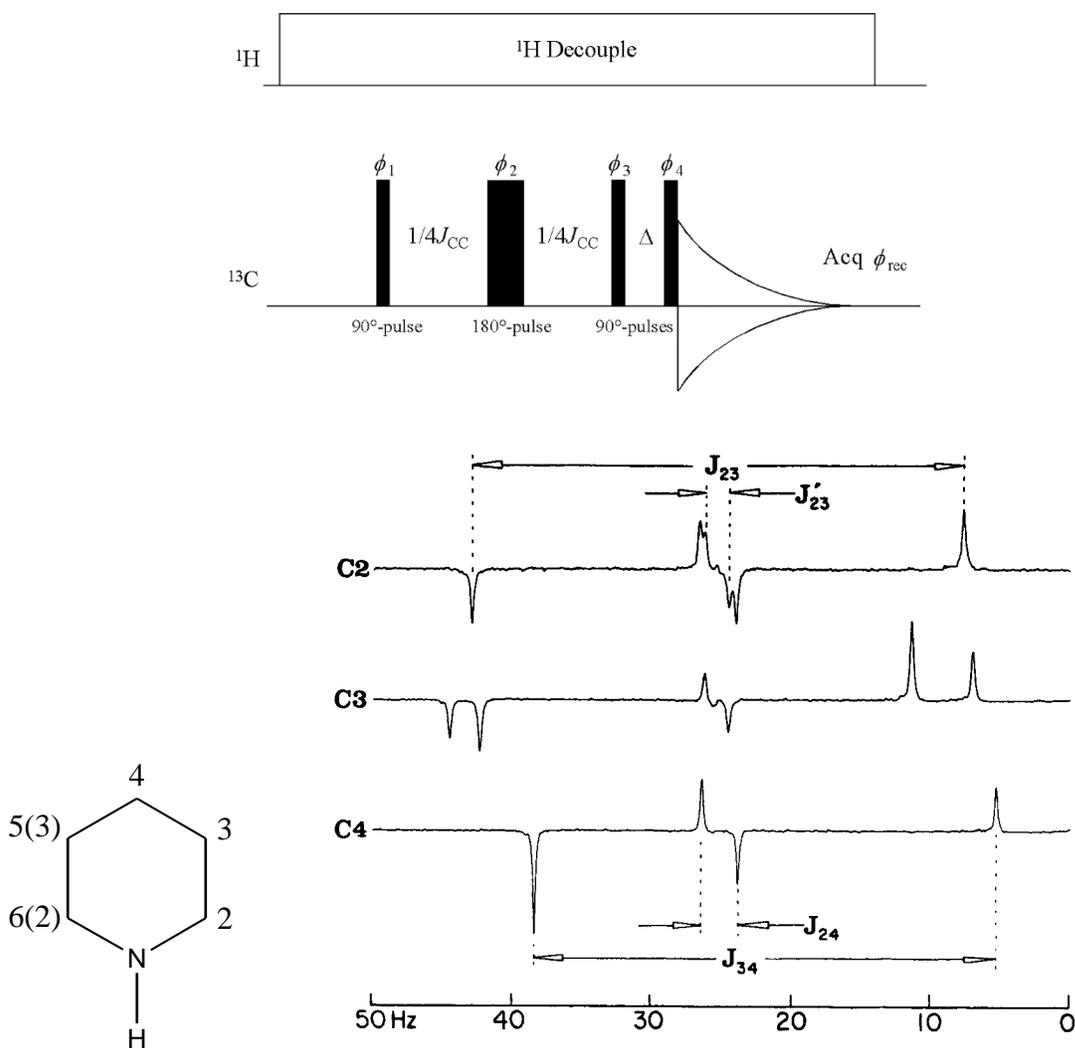The pulse sequence for the 1D INADEQUATE experiment is shown below:

Figure 2 from Bax et al., (1980).

The J_{CC} coupling constants for piperidine are measured to be:

$$^1J_{23} = 35.2 \text{ Hz, } ^3J_{23'} = 1.7 \text{ Hz, } ^2J_{24} = 2.6 \text{ Hz and } ^1J_{34} = 33.0 \text{ Hz}$$

The delay $1/4J_{CC}$ is generally optimized for $^1J_{CC}$, i.e., 35 Hz, in which case the delay is set to be approximately 7 ms. Nevertheless, geminal and vicinal coupling are also observed.

The INADEQUATE experiment may also be recorded as a 2D experiment as shown below:
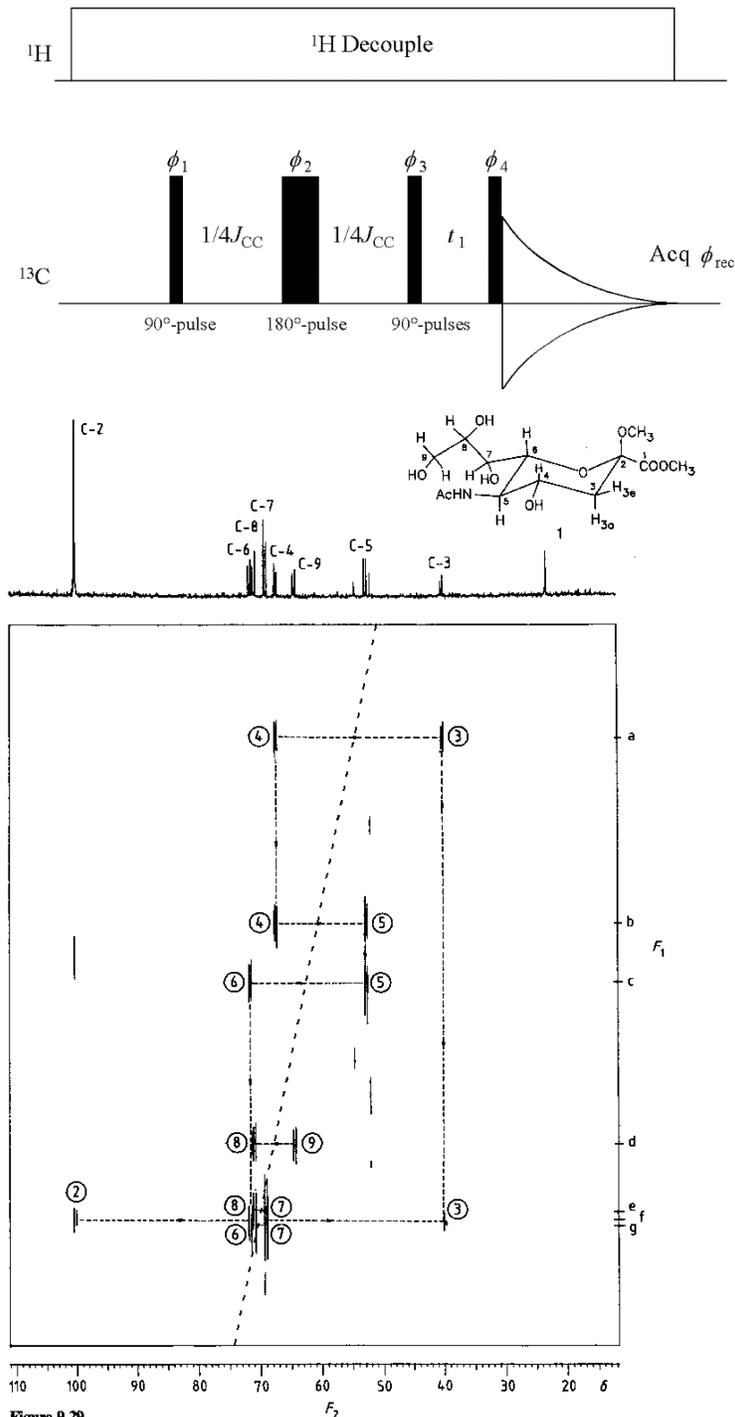

Figure 9-29.

A portion (δ = 10 to 110) of the two-dimensional 100.6 MHz ^{13}C INADEQUATE spectrum, with ^{1}H BB decoupling, of the neuraminic acid derivative 1. The projection of the 2D spectrum onto the F_2-axis is shown at the top. The horizontal construction lines link the doublets of coupled pairs of ^{13}C nuclei. The identification numbers alongside the signals correspond to the numbering of the carbon atoms in 1. Starting from C-2 and following the horizontal and vertical construction lines in the direction of the arrows leads to unambiguous assignments of all the ^{13}C resonances.

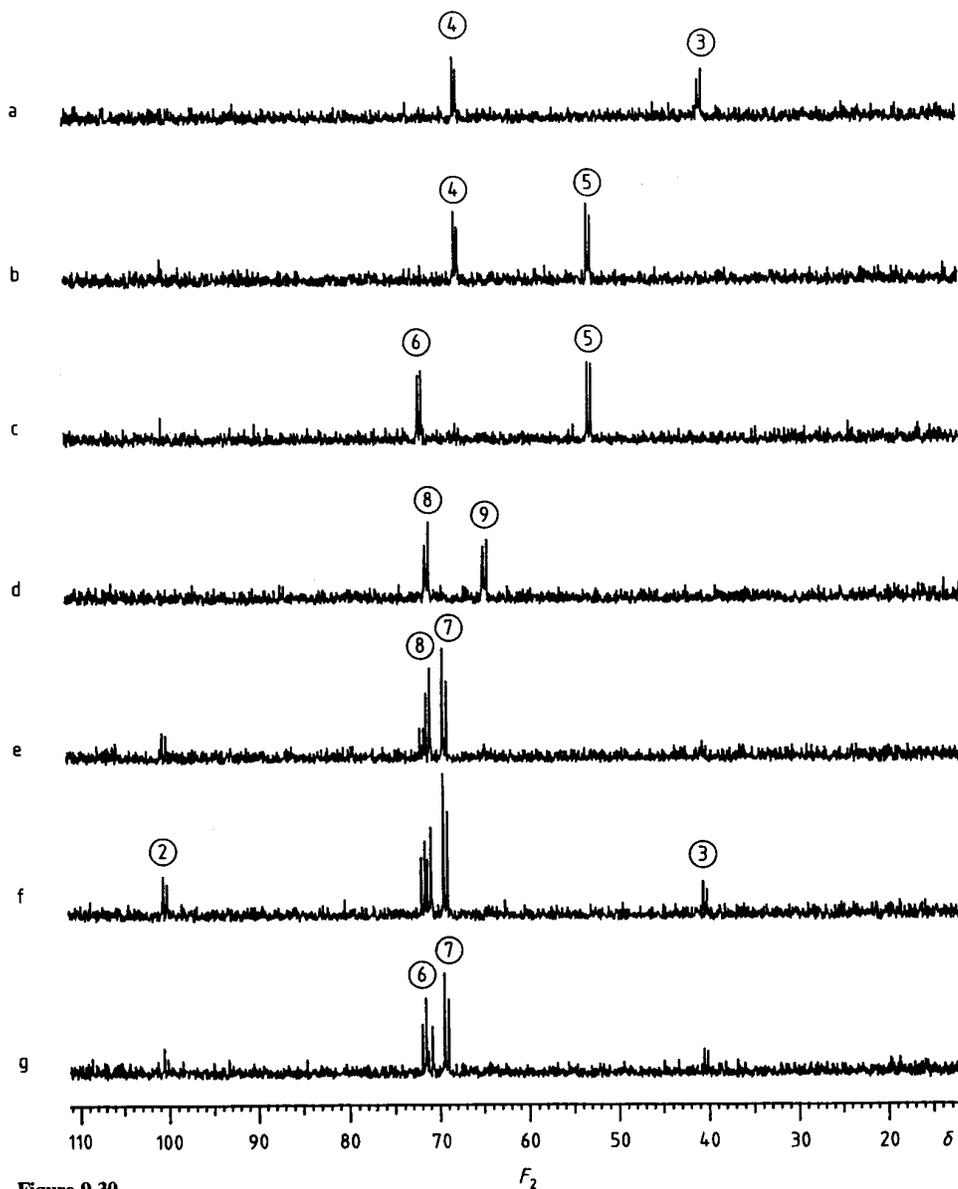**Figure 9-29 from the Friebolin text.**

Figure 9-30.

Individual F_2-spectra for a series of different F_1-values from the 2D-INADEQUATE experiment on **1**. The traces a to g have been chosen so that in each case an AB- or AX-type satellite spectrum for a coupled pair of ^{13}C nuclei is visible. The F_1-values for spectra a to g are indicated on the axis in Figure 9-29. It is evident from traces e, f and g that the resolution along the F_1-axis is not quite adequate to completely separate the 2/3, 6/7 and 7/8 pairs.
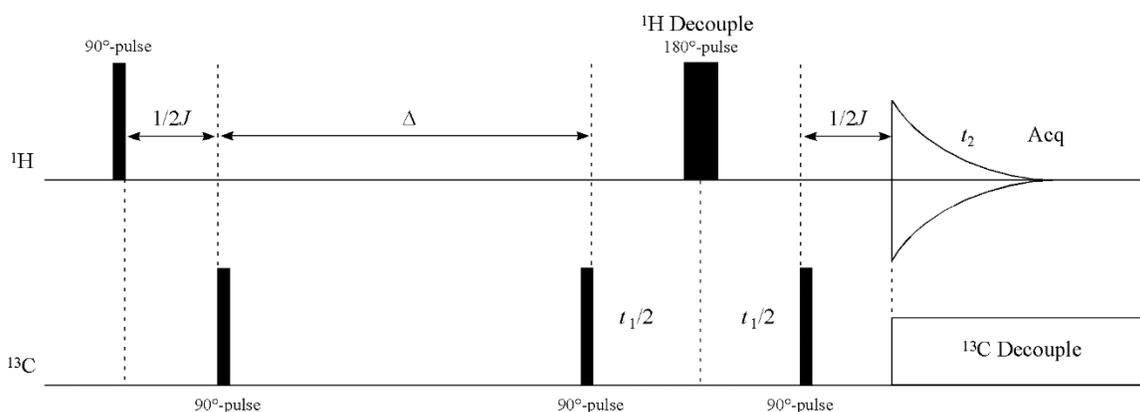
(*Experimental conditions:*
167 mg of the compound in 2.3 ml D_2O; 10 mm sample tube; 128 measurements with t_1 altered in 50 μs increments; each measurement with 576 FIDs; total time 66 h.)

INADEQUATE data can provide key structural insights, however the method has very low relative sensitivity, i.e., ^{1}H{^{13}C} NOE enhancement with direct ^{13}C detection, and application of the approach requires sample concentrations above 100 mM.

4

HMBC: Heteronuclear Multiple-Bond Correlation Spectroscopy

The HMBC experiment is a powerful variant of the HMQC method can produce so-called multiple bond (C–C) correlations between ^{1}H and remote heteronuclei:

$$^1\text{H}-^{13}\text{C}-^{13}\text{C}-^{12}\text{C}-^{12}\text{C}$$

$$^1\text{H}-^{13}\text{C}-^{12}\text{C}-^{13}\text{C}-^{12}\text{C}$$

$$^1\text{H}-^{13}\text{C}-^{12}\text{C}-^{12}\text{C}-^{13}\text{C}$$
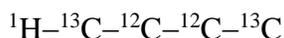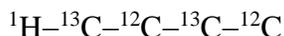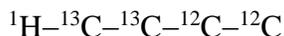
The method provides correlation between ^{13}C separated by one- two- or three bonds with high relative sensitivity since it incorporates both polarization transfer and ^{1}H-detection.

The interval specified by $1/2J$ represents the standard interval in the HMQC spectrum employed to produce antiphase coherence:

$$\frac{1}{2J} = \frac{1}{2(140\text{ Hz})} \approx 0.0036\,\text{sec}$$

Recall that full antiphase coherence character is produced when the components of the ^{1}H vector that are coupled to the α and β states of the ^{13}C spins are 180° apart from one another.

In practice for this $1/2J$ interval may be varied between 3 ms and 5 ms depending on J_{CC} and the T_2 of the ^{13}C spins.

The geminal, $^2J_{CC}$, and vicinal, $^3J_{CC}$, couplings are substantially smaller than the direct coupling, i.e., < 5 Hz versus 30-40 Hz.

Since the development of antiphase character develops much more slowly for these smaller couplings, the first ^{13}C 90°-pulse has little affect on the state of the system, whereas the antiphase state for the coupled spins is converted in a multiple quantum manifold:
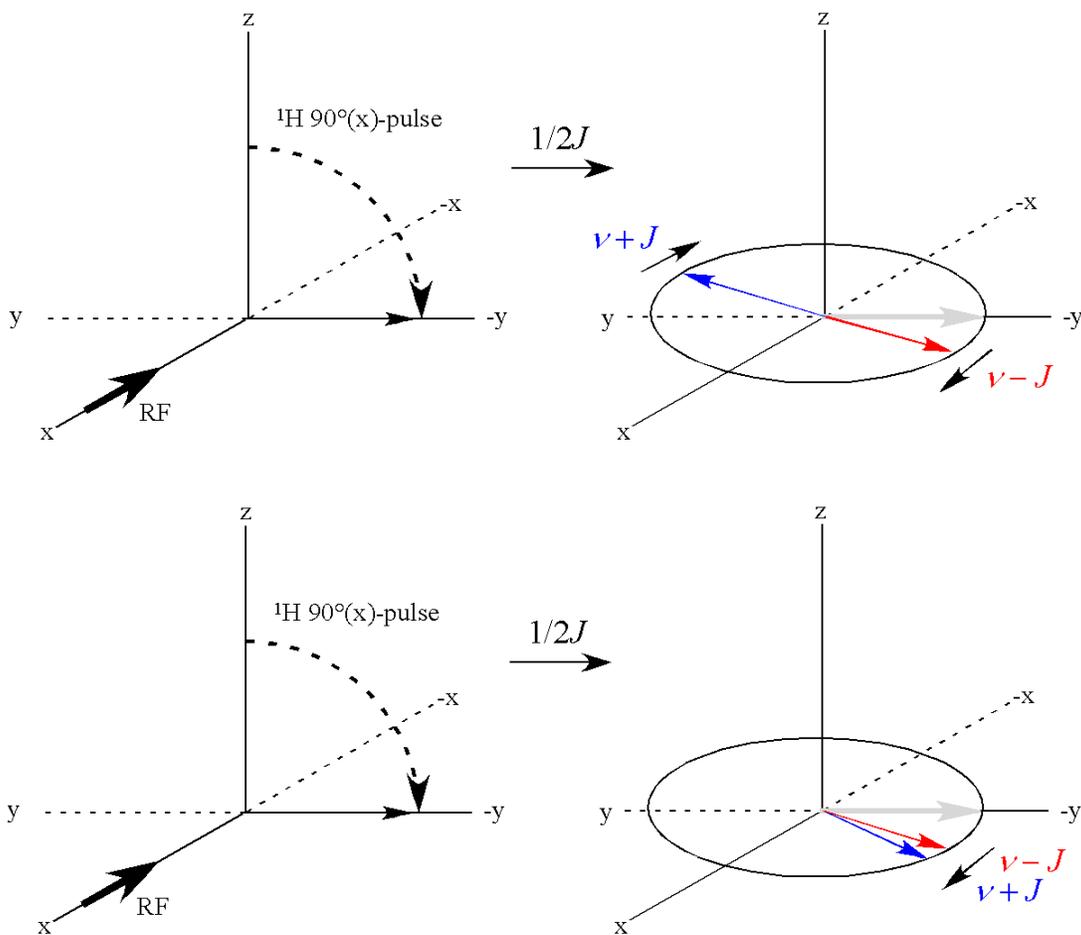
This difference may be exploited to eliminate signals arising from directly coupled spins using the same sort of approach that was used to eliminate uncoupled ^1H signals from the HMQC experiment. In this context the technique is know as a *low-pass filter* since only signals from lower frequency components survive the sequence.

Figure 1 from Bax, A. and Summers, M.F. (1980) ^{1}H and ^{13}C Assignments from Sensitivity-Enhanced Detection of Heteronuclear Multiple-Bond Connectivity by 2D Multiple Quantum NMR. *J. Am. Chem. Soc.* **108**, 2093-2094.
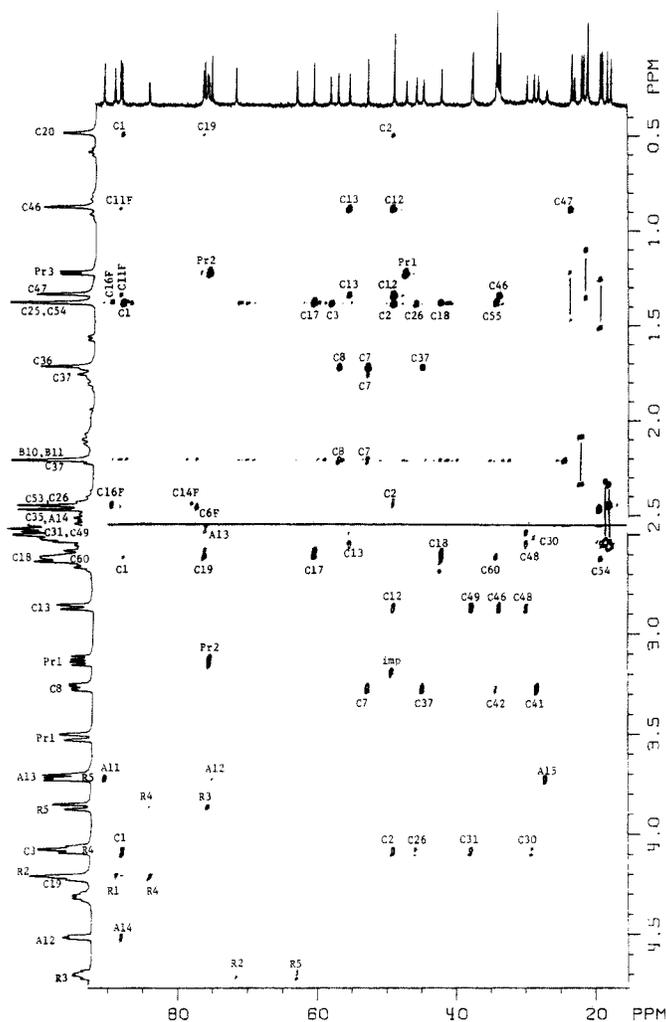

Figure 1. High-field region of the 500-MHz absolute value mode ^{1}H–^{13}C long-range correlation spectrum of a sample of 4 mg of coenzyme B_{12}, dissolved in 0.35 mL of D_2O. The measuring time was 15 h. The lowest contour level in the upper half of the spectrum (above the drawn line) has been chosen 3 times higher than for the lower half, because, at lower contour levels, t_1 noise from the intense methyl signals starts obscuring the connectivities of interest. At the top of the spectrum, the conventional ^{1}H-decoupled ^{13}C spectrum recorded on a JEOL GX400 spectrometer (using 50 mg of sample) is shown. Incompletely suppressed direct correlations, marked by vertical bars, are observed for the methyl groups C53, C35, B10, B11, C54, C25, C47, and Pr3.[15] Resonances that are folded in the ^{13}C dimension are labeled "F".

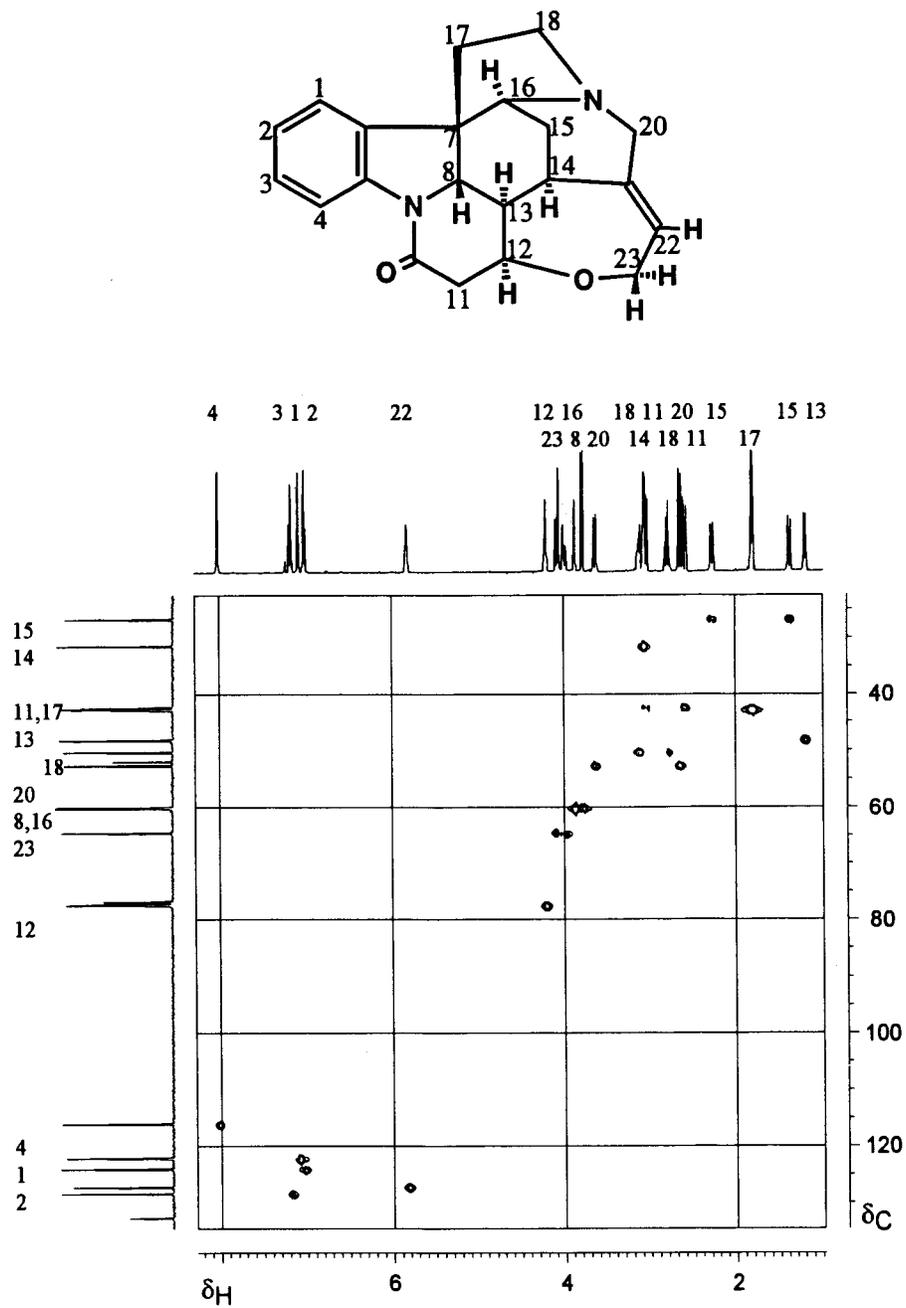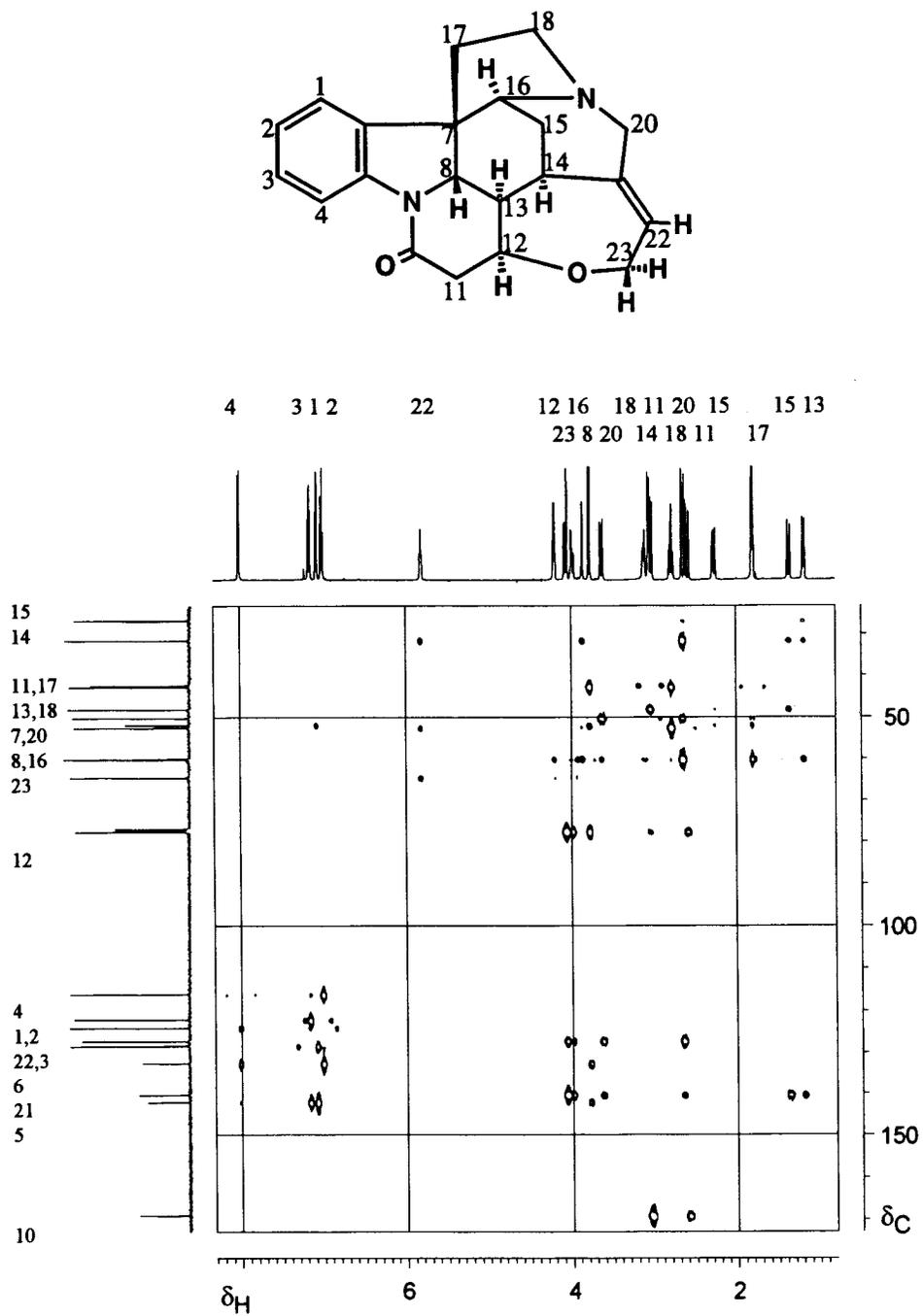gs-HMQC of strychnine at 500 MHz ^{1}H:

Figure 12.3 from Braun, S., Kalinowski, H.O. and Berger, S. (1998) *150 and More Basic NMR Experiments.* **Wiley-VCH, New York.**

gs-HMBC of strychnine at 500 MHz ^{1}H:

3D Multinuclear experiments

3D HMQC-COSY: This experiment resolves ^{13}C in F1, ^{1}H in F2 and ^{1}H in F3. The F1-F2 planes correspond to a HMQC experiment, while the F2-F3 planes correspond to a COSY experiment. The transfer pathway is given as follows:

$$H_z \longrightarrow H_{xy} \xrightarrow{1/2J} C_{xy}[t_1] \xrightarrow{1/2J} H_{xy}[t_2] \longrightarrow H_{xy}[t_3]$$
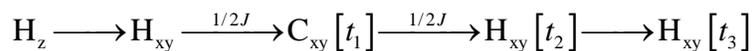
wherein the correlations produced post-HMQC are restricted to COSY-like transfers, i.e., geminal and vicinal ^{1}H couplings.

a: H,H plane at δ_C = 42.5

10

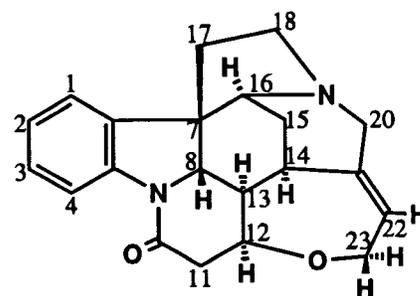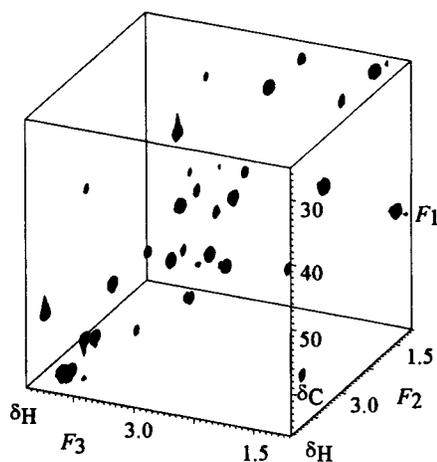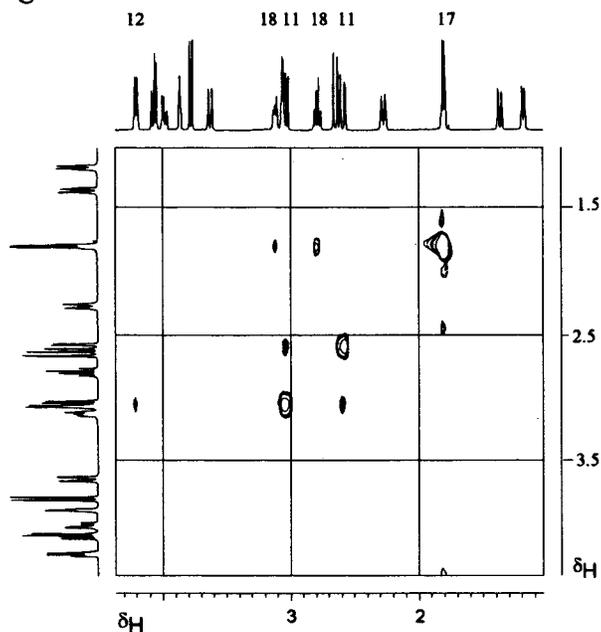3D HMQC-TOCSY: This experiment resolves ^{13}C in F1, ^{1}H in F2 and ^{1}H in F3. The F1-F2 planes correspond to a HMQC experiment, while the F2-F3 planes correspond to a COSY experiment. The generic transfer pathway is given as follows:

$$H_z \longrightarrow H_{xy} \xrightarrow{1/2J} C_{xy}\left[t_1\right] \xrightarrow{1/2J} H_{xy}\left[t_2\right] \longrightarrow H_{xy}\left[t_3\right]$$

wherein long-range ^{1}H-^{1}H correlations are produced.

a: H,H plane at δ_C = 26.7

Pulsed Field Gradients: Theory and Application

Barker, P. and Freeman, R. (1984) Pulse Field Gradients in NMR. An Alternative to Phase Cycling. *J. Magn. Reson.* **64**, 334-338.

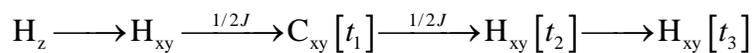Thus far we have considered two very distinct types of magnetic fields: The static (Zeeman) field that produces the bulk polarization and a time-dependent field, i.e., RF pulses. We now consider a magnetic field that is both temporally and spacially dependent.

We can also generate a magnetic field that may be gated, i.e., rapidly turned on and off, and which varies in strength across the sample chamber

The object of the PFG is to install a magnetic field gradient across the sample which adds/subtracts to the main (static) field, $\mathbf{B}_0$ in a coordinate-dependent fashion. During the gradient pulse spins in different locations experience different net magnetic field vectors.

The apparatus used to generate the field--gradient pulse may be diagrammed as shown below (from Barker and Freeman (1985)):

FIG. 1. (a) The geometrical arrangement of the field gradient coils with respect to the radiofrequency NMR coil (shown for simplicity without input leads). (b) Switching circuitry for reversing the polarity of the gradient coils and for damping the ringing after the pulses. During the gradient pulse either the field effect transistors F1 and F4, or F2 and F3, are conducting; after the pulse F3 and F4 are conducting.

Figure 1 from Barker and Freeman (1984).

The effects of the PFG may be demonstrated using the simple pulse sequence shown below:

$$90°$$

¹H

G$_z$
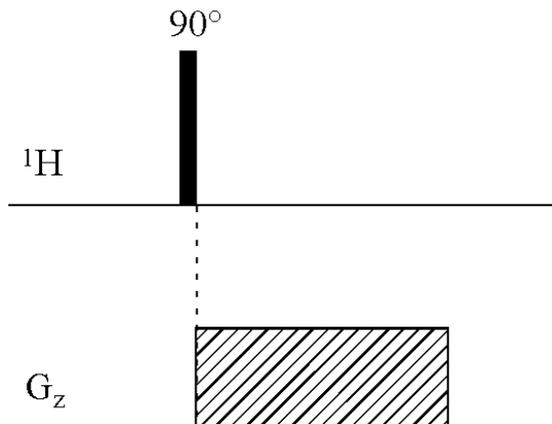
Field gradient pulses are characterized by intensity (flux density), duration, and shape (i.e., rectangular, sine-bell, Gaussian, etc.).

From Barker and Freeman (1985):

> `...The principal attribute of the field--gradient technique is the ability to speed up experiments where the inherent sensitivity is so high that time averaging is unnecessary. However [sic], many phase-cycling schemes have now become so complicated (through the nesting of many independent cycles) that programming errors can easily arise, with dramatic losses in signal intensity. Gradient pulses seem easier to implement...'.

A dramatic statement given that the PFG apparatus in this case was 'home-built'.

The net effect of the PFG is to make the Larmor precession frequencies position dependent. Consider:

Free-Precession

$$\omega = \gamma B_0$$

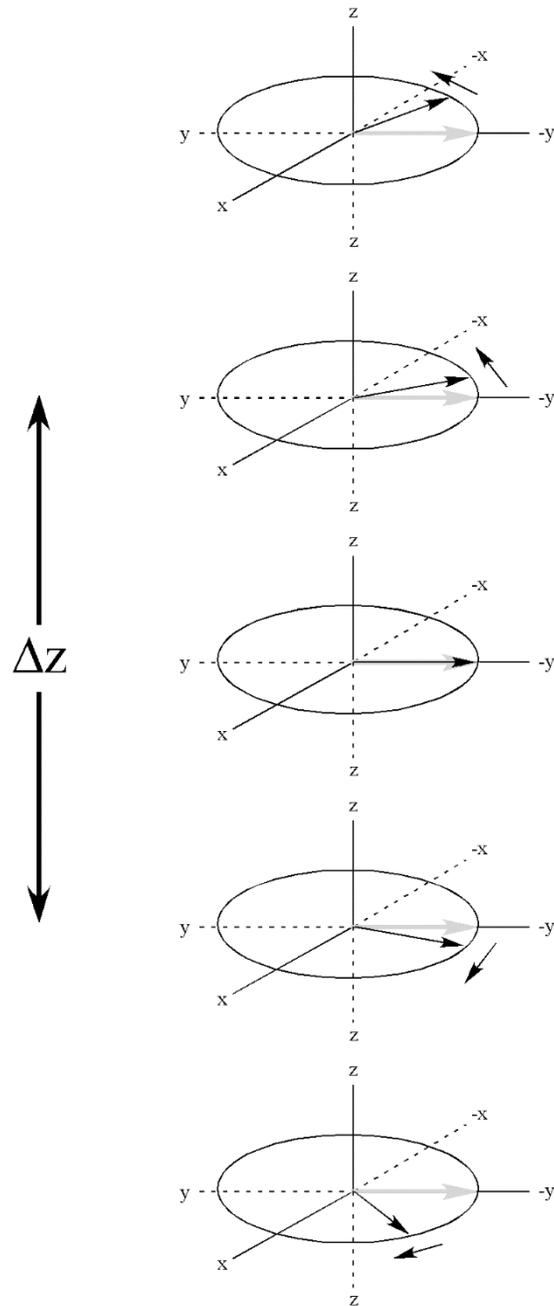Chemical Shift

$$\omega = \gamma (1 - \sigma) B_0$$

PFG

$$\omega = \gamma (1 - \sigma) B_0 + \gamma (1 - \sigma) \Delta B_0 r_z$$

Since $|\sigma| \ll 1$ and $\Delta B_0 r_z \approx \left(30 \text{ G cm}^{-1}\right)\left(1.5 \text{ cm}\right) \ll B_0 \approx 10^4 \text{ G}$, we may accept the approximation that $\sigma \Delta B \rightarrow 0$ and therefore that

$$\omega \cong \gamma\left(1-\sigma\right)B_0 + \gamma \Delta B r_z$$

The effects may be diagrammed as shown below:

The PFG causes transverse magnetization at a particular position within the sample volume to rotate through angle that depends upon the gyromagnetic ratio of the spin, the strength of the PFG (in Gauss) and the position.

The strength of the PFG is set so that for a given sample volume and duration, spins are rotated through several cycles, thus completely scrambling the magnetization over the sample volume.

Such a condition is known as a *z-coil* since the spin vectors are rotated in a highly consistent pattern along the z-axis

Since for every vector in a z-coil there is a vector somewhere in the sample volume that points in the exact opposite direction, the sum of the vectors over the sample is zero. The transverse magnetization may thus be effectively eliminated by a PFG element.

Note that if we apply a PFG of a given strength for a specified interval, we can actually retrieve the original state by applying a PFG of the same strength (+) and duration but in the opposite sense (−). The second PFG will unwind the effects of the first PFG.